

# LEARNING DEEP TEMPORAL REPRESENTATIONS FOR BRAIN DECODING

**Orhan Firat, Emre Aksan & Fatos T. Yarman Vural**

Department of Computer Engineering

Middle East Technical University

Ankara, Turkey

{orhan.firat, eaksan, vural}@ceng.metu.edu.tr

**Ilke Oztekin**

Department of Psychology

Koc University

Istanbul, Turkey

ioztekin@ku.edu.tr

## ABSTRACT

Functional magnetic resonance imaging produces high dimensional data, with a less than ideal number of labelled samples for brain decoding tasks. In this study, we propose a deep temporal convolutional neural network architecture for brain decoding task in order to reduce dimensionality of feature space along with improved classification performance. Temporal representations (filters) for each layer of the convolutional model are learned by leveraging unlabelled fMRI data in an unsupervised fashion by employing regularized autoencoders. Learned temporal representations in multiple levels capture the regularities in the temporal domain and are observed to be a rich bank of activation patterns which also exhibit similarities to the actual hemodynamic responses. Further spatial pooling layers in the convolutional architecture reduce the dimensionality without losing excessive information. By employing the proposed temporal convolutional architecture, raw input fMRI data is mapped to a non-linear, highly-expressive and low-dimensional feature space where the final classification is conducted. In addition, we propose a simple heuristic approach for hyper-parameter tuning when no validation data is available. Proposed method is tested on a ten class recognition memory experiment with nine subjects. The results support the efficiency and potential of the proposed model, compared to the baseline multi-voxel pattern analysis techniques.

## 1 INTRODUCTION

Brain decoding using functional magnetic resonance imaging (fMRI) is a challenging problem that has received much attention recently. The major difficulty for the machine learning tasks using fMRI data is the scarcity of labelled samples compared to the high dimensional input spaces. In a typical task related fMRI experiment, the number of labelled samples over several time points reaches at most hundreds but the dimension of the input space (number of voxels) easily exceeds thousands even a small region of interest is considered. Therefore a great deal of effort spent to either reducing the dimensionality Viviani et al. (2005); Sidhu et al. (2012) or employing spatial/temporal structures Battle et al. (2006); Pereira & Botvinick (2011) in order to improve classification accuracy and significance. As a result, many brain decoding systems rely on cleverly hand-crafted features Norman et al. (2006); Haynes & Rees (2006); Shirer et al. (2012) to represent cognitive processes. Another issue related to the low number of labelled samples is the labelling processes which is strongly coupled with the experimental design. Within the time points acquired during an experiment, only few are assigned to corresponding class labels by considering the timing of the stimulus. For example in a block design, a predetermined number of time points are averaged within a block to obtain a smoothed intensity value Mitchell et al. (2008) and assigned to a class label. Similarly in an event

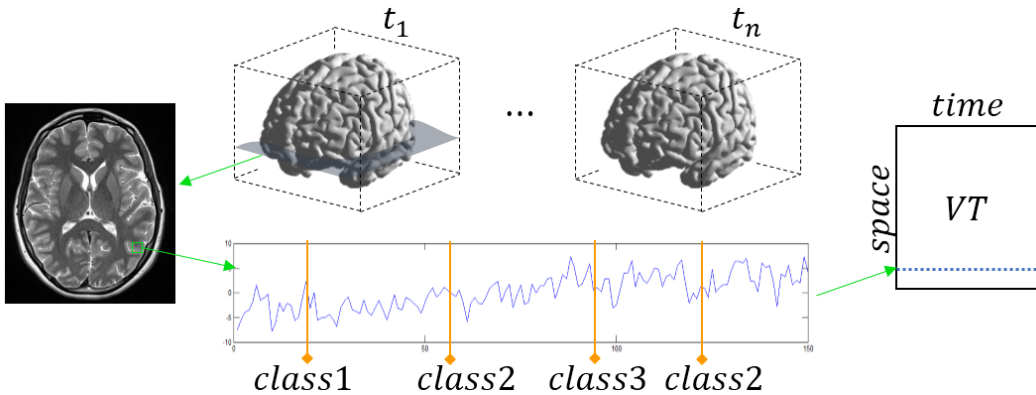


Figure 1: Example of a typical fMRI experiment for brain decoding. 4-dimensional fMRI data consists of several volumes across time, some of which are assigned to a class label.

related design, class label is assigned to time points according to the prior knowledge of the peaks of hemo-dynamic response function (e.g. 2-3 time points after the stimulus) Norman et al. (2006); Oztekin & Badre (2011). The rest of the unlabelled samples are generally thrown away and not used further in the decoding tasks.

Recent improvements in unsupervised feature learning and transfer learning points out the importance of employing unlabelled data for a better classification Raina et al. (2007); Erhan et al. (2010). Learning the data generating distribution  $p(x)$  by leveraging unlabelled data improves further discriminative tasks  $p(y|x)$ , when  $p(x)$  and  $p(y|x)$  share some structure Bengio et al. (2013). In this study we hypothesize that the discarded unlabelled samples of an experiment still contains useful information considering the temporal and spatial structure, and can be used efficiently for brain decoding tasks.

In this paper, we attack the brain decoding problem from both dimensionality reduction and leveraging unlabelled data perspectives for an improved classification accuracy. In order to represent noisy and redundant fMRI data, we use an unsupervised feature learning algorithm that can automatically extract multiple levels of temporal features using both labelled and unlabelled data. Such approaches are common in computer vision Le et al. (2011) but have not adapted for neuroimaging data especially for brain decoding. By incorporating unlabelled data and very little prior knowledge, we learn two levels of temporal filters for fMRI data representation without hand-crafting them. Further we integrate learned temporal representations into a deep temporal convolutional neural network (CNN). CNNs have demonstrated many successes recently Krizhevsky et al. and have potential to enhance models for brain decoding. We employ learned temporal representations to capture the temporal information by convolution and then use spatial pooling within CNN layers to reduce dimensionality. By leveraging unlabelled data and the representational power of CNNs, we are able to train robust classifiers. The constructed feature spaces are automatically formed by temporal representations and have a reduced dimensionality thanks to spatial pooling. The proposed method substantially improves classical and enhanced multi-voxel pattern analysis (MVPA) methods for brain decoding on a recognition memory experiment with nine participants.

## 2 UNSUPERVISED LEARNING OF TEMPORAL REPRESENTATIONS AND CONVOLUTIONAL ARCHITECTURE

In this section, we describe proposed unsupervised learning architecture for deep temporal representations. fMRI data is composed of 3-dimensional brain volumes across time  $\{t_i\}_{i=1}^n$ , where each 3D volume is formed by stacking several 2D slices (scans) and  $n$  is the total length of the experiment across runs (see Figure 1). Each pixel in these 2D images are actually represents the intensity of a small volume of brain tissue (voxel) at a time instant  $t_i$ . The intensity value of a voxel at location  $j$  at a time instant  $i$  can be denoted as  $v_i^j$ , where  $j = 1, \dots, m$  and  $m$  is the total number of voxels in the experiment. A typical fMRI experiment consists of several runs, where in each run the subject is

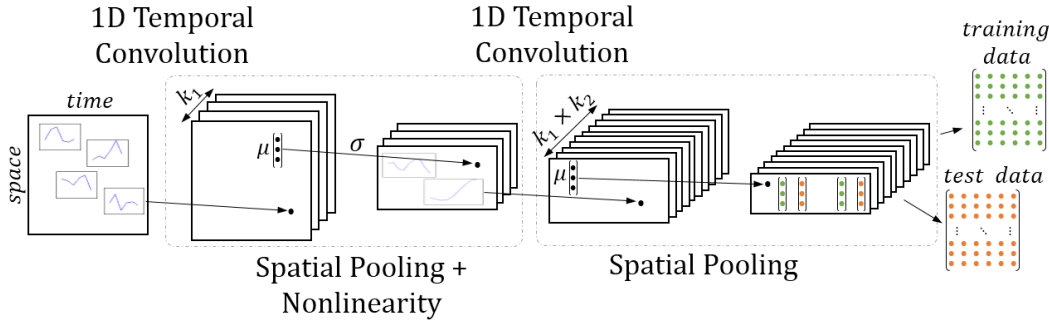


Figure 2: Temporal Convolutional Neural Network used for brain decoding.

exposed to some task specific stimulus at the predefined time instants. Each of these stimulus corresponds to a class and the data acquired at that instant is assigned to corresponding class label (orange vertical lines in Figure 1). The entire experimental data can be represented by a voxel  $\times$  time matrix  $VT$ , where columns are representing the brain volumes in terms of voxels (space), the rows stand for voxel time series (time). Further in the classification labelled samples are separated into two sets, where the first set is employed in training the classifier and the second set is used for generalization test. Conventional MVPA methods discard the columns of  $VT$  that do not have class labels and represent cognitive states by using voxel intensity values as features. Although the discarded data do not carry label information, it carries the temporal structure (activation pattern) of each voxel across time. In order to improve representation power of features, it is promising to capture this structure and employ them as a substitute for raw intensity values.

In this study we use the entire  $VT$  matrix (except the columns separated for test) to learn temporal filters in two layers. Our aim is to learn a number of activation patterns that are able to reflect temporal regularities in the data without hand-crafting them. For learning temporal filters in an unsupervised fashion we employ sparse autoencoders Kavukcuoglu et al. (2009). An autoencoder is a neural network trained by back-propagation which attempts to reconstruct its input by setting the target values to be equal to the inputs,  $x \approx \tilde{x}$ . Let  $x$  be the dataset of time windows of length  $\tau_1$  that are sampled from the rows of the  $VT$  randomly. Autoencoder consists of two consecutive functions, first an encoder function  $f_{\theta_1}(x)$  applied on  $x$  with parameters  $\theta_1$  which maps  $x$  to a hidden representation  $h$ . The second function is the decoder function  $g_{\theta_2}(f_{\theta_1}(x))$  which maps the hidden representations to the reconstruction  $\tilde{x}$  with parameters  $\theta_2$ . By enforcing a sparsity constraint (activation around zero) to hidden layer neurons via the cost function, autoencoder learns a compact and non-linear representation of its input  $x$ . The number of hidden neurons is equal to the number of filters to be learned and set  $k_1$  for the first layer temporal representations. The sparse autoencoder having  $k_1$  hidden neurons is trained to minimize reconstruction error using back-propagation by minimizing the following cost function,

$$J_{\text{sparse}}(\Theta) = J_{NN}(\Theta) + \beta J_{\hat{\rho}} + \lambda \|\Theta\|_2^2, \quad (1)$$

where  $J_{NN} = \frac{1}{2} \sum_i \|\tilde{x}^{(i)} - x^{(i)}\|_2^2$  is the neural network reconstruction term and  $\lambda \|\Theta\|_2^2$  is the L2 regularization term on parameters and  $\beta$  is the hyper-parameter controlling the importance of sparsity in the model. Sparsity term  $J_{\hat{\rho}}$  is the crucial term in our autoencoder. Let  $a(\cdot)$  be the sigmoid activation function and  $\hat{\rho}_j = \mathbb{E}[a_j(x)]$  be the expected activation of hidden unit  $j$  over the dataset. By enforcing the constraint  $\hat{\rho}_j = \rho$  where  $\rho$  is the sparsity hyper-parameter, hidden layer activations can be adjusted to be sparse. In order to measure the sparsity cost, Kullback-Leibler divergence between average activation of a unit  $\hat{\rho}$  and sparsity parameter  $\rho$  is calculated as  $J_{\hat{\rho}} = \sum_j^{k_1} KL(\rho \parallel \hat{\rho}_j)$ . The optimization of the cost function (1) yields the model parameters  $\Theta = \{\theta_1, \theta_2\}$  and columns of the transition weights  $\theta_1$  of encoder function  $f_{\theta_1}(x)$ , constitutes the temporal filters. After learning  $k_1$  number of filters in the first layer, all the  $VT$  matrix is convolved along the time axis (1D full temporal convolution) with the learned filters and  $k_1$  number of response matrices extracted. Note that, resulting response matrices are the same size as  $VT$  with a full convolution.

In a convolutional neural network, a general processing block is constructed by three consecutive operations; convolution, pooling and applying an element-wise non-linearity Krizhevsky et al.. Further these blocks can be repeated consecutively feeding output of one block to the next one Le et al. (2011). We construct our temporal convolutional model with two processing blocks as shown in Figure 2 with dashed boxes. To complete our first processing block we determine a spatial pooling function  $\mu$ , a pooling range in a vicinity  $\delta_1$  and point-wise non-linearity function  $\sigma$ . Considering the capillary structure of the brain and point spread function of fMRI medium, it is expected that nearby voxels exhibit correlated activations Pereira & Botvinick (2011). Therefore for the choice of  $\mu$  we employ max pooling on the columns of response matrices. Note that, the columns of the response matrices correspond to spatial domain of fMRI data and as we increase the pooling range without any overlaps between pooling functions, the final dimensionality decreases. As an example, a spatial pooling range  $\delta_1 = 2$  with  $m$  rows (voxels) and  $n$  columns (time points) response matrix results in an  $m/2$  rows and  $n$  columnned pooled response matrix where the maximum of each of 2 closest voxel responses are taken<sup>1</sup>. We finalize the first processing block by applying  $\sigma$ , which is set to hyperbolic tangent, to all elements of the pooled response matrices.

The second level of our deep temporal convolutional net takes the pooled response matrices as input and repeats the same pipeline conducted in the first block. The only difference for the second block is the number of input matrices, which is  $k_1$  number of  $m/\delta_1$  rowed and  $t$  columnned pooled response matrices. For each of these matrices a separate  $k_2$  number of temporal filters are learned again by employing sparse autoencoders but one autoencoder for each. Same procedure is followed  $k_1$  times, by first collecting  $\tau_2$  length time windows from the rows of an input response matrix then training a sparse autoencoder having  $k_2$  number of hidden units. Each  $k_2$  filters are then convolved with the corresponding first level pooled response matrix. Repeating this process for all inputs of the second block then applying pooling and non-linearity similarly, we obtain  $k_1 \times k_2$  number of second level pooled response matrices. Note that second level pooled response matrices have  $m/(\delta_1 \times \delta_2)$  rows and  $t$  columns, where  $\delta_2$  is the pooling range for second processing block. As mentioned above, the class labels are carried along the columns of the initial  $VT$  matrix. After processing raw input data with the proposed temporal convolutional model, resulting second level pooled response matrices have the same number of columns  $t$ , hence still carries the class label information. Finally at this point, all the second level pooled response matrices are concatenated along their time axis resulting our final representation matrix which has  $(m \times k_2)/(\delta_1 \times \delta_2)$  rows and  $t$  columns. We separate the training and test data by extracting corresponding columns according to the experiment design class labels.

### 3 EXPERIMENTS ON FMRI DATA

fMRI recording was conducted during a recognition memory task on nine participants. Each participant is shown a list of words belonging to a specified category in the encoding phase within ten categories (e.g. fruits or tools). Following a delay period where the participant solves mathematical problems a test probe is presented and the participant executes a yes/no response indicating whether the word belongs to the current study list (e.g., see Oztekin & Badre (2011)). For the decoding task we focused on a sub-region of lateral temporal cortex region having 1024 voxels. fMRI data consists of 2400 time points in 8 runs, with 240 class labels for the encoding phase and 240 class labels for the retrieval phase (for each of ten classes, 24 samples for both encoding and retrieval). The classification task we seek to accomplish is to predict class labels of the samples in the retrieval phase by using samples in the encoding phase. Measurements recorded in the encoding phase are used as labelled training samples and measurements in the retrieval phase are used as test samples. The recording was conducted using a 3T Siemens scanner with a 2 seconds TR, meaning that we obtained a separate brain volume each 2 seconds. Apart from slice-scan time correction, 3D motion correction and registration, no additional pre-processing was employed.

#### 3.1 MODEL DETAILS

The proposed model is tested using fMRI experiment data with various architectural choices. Our main consideration was to reduce the final representation dimensions with increased pooling ranges.

<sup>1</sup>Pooling functions are applied to closest voxel pairs in the 3D-brain volume, not in the consecutive elements of  $VT$  matrix columns. Pooling regions in Figure 2 are drawn for the ease of understanding.

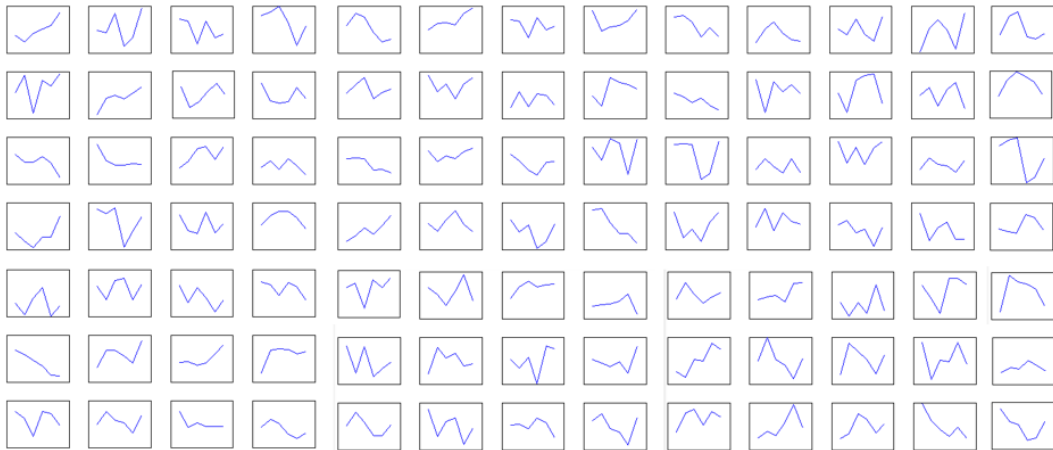


Figure 3: A collection of the first level temporal filters learned from unlabelled data across different subjects. Each small box represents a temporal filter. Filters are randomly chosen across all subjects.

For this purpose, we adjusted the pooling ranges  $\delta_1$  and  $\delta_2$  to retract number of dimensions comparable with the standard MVPA method (which is equal to number of voxels) and even lower. Considering the experimental protocol TR as 2sec, a full HRF could be captured with a temporal window size of 6 samples. Therefore the sampling window length of the first block  $\tau_1$ , is set to 6. It is common for CNNs that the higher level receptive fields gets wider to capture more abstract regularities Krizhevsky et al., so we increased the second block temporal sampling window length  $\tau_2$ , to 9 samples (7-10 range give similar results). Note that, the collected windows that overlap with the test samples are discarded for fairness.

A major strait of CNNs and many other deep learning methods, is the large number of hyper-parameters to be tuned Bengio et al. (2013). Without a proper cross-validation set, as in our case, these hyper parameters are left to be tuned with trial and error fashion which we avoided in this study. For the hyper-parameters of the autoencoders in both levels  $k_1, k_2, \beta, \rho, \lambda$ , we propose following numerical quality assurance. It is obvious that the hidden representations of an autoencoder are expected to learn different regularities from the input, hence, the representation power is increased as the learned filters are decorrelated. We searched in a random parameter search space for these hyper-parameter combinations. For each learned filter bank with a combination, we calculated the correlation matrix of learned filters. In fully decorrelated case, the diagonalized correlation matrix should be close to the identity matrix hence we calculated the L1 distance between them. We determine the hyper-parameter combination having the lowest distance, as  $k_1 = 16, k_2 = 4$ . The first layer temporal representation are illustrated in Figure 3, where we observe several HRF alike filters. Moreover, the filters learned directly from unlabelled data are capable of representing several other activation patterns such as linear trends, boxcar, rapid dips and peaks, even some baseline trends. The proposed model takes raw fMRI intensity values as input without any normalization or pre-processing such as whitening or z-scores. Using linear activations at the output layer of autoencoders makes it possible to learn representations for datasets not in range 0-1.

### 3.2 TESTING PROCEDURES AND COMPARISON

For the validity of the proposed model, we map the raw input fMRI data into the learned representation space with our pre-trained temporal CNN. Further, in the representation space, training and test samples are extracted and final design matrix is formed for classification. In order to compare proposed method with other MVPA methods, we employ a k-nearest neighbor classifier for all methods. For the proposed model, we also evaluate a single level temporal convolutional network to monitor the impact of the depth. Three different MVPA approaches are taken into consideration. The baseline is Raw MVPA method where raw intensity values are directly fed to classifier. To make a fair comparison we further employ temporal information to classical MVPA method in two different ways. First, we convolved the raw intensity values with a double gamma HRF function adjusted to span 6 samples to account for temporal activation pattern in a hand-crafted way, which we called

Table 1: Classification performance of the proposed method.

Method	$\delta_1$	$\delta_2$	Sub1	Sub2	Sub3	Sub4	Sub5	Sub6	Sub7	Sub8	Sub9	Dim
Raw MVPA	-	-	28,9	41,5	43,1	45,5	42,3	31,9	34,0	40,6	41,4	1024
HRF MVPA	-	-	32,3	44,4	42,3	53,8	36,1	41,1	44,5	46,5	48,2	1024
T-MVPA	-	-	41,9	52,4	52,0	53,9	45,3	44,0	44,9	51,1	52,5	6144
Single Layer	2	-	54,0	65,7	65,3	67,8	66,7	64,1	66,1	65,7	69,5	8192
Single Layer	4	-	56,1	64,5	63,6	69,5	66,2	65,3	66,1	66,5	68,6	4096
Single Layer	8	-	55,7	65,3	62,8	69,5	64,0	64,9	66,1	67,4	70,0	2028
Single Layer	16	-	51,9	64,0	63,2	68,6	62,3	63,3	64,9	67,3	67,0	1024
Two Layers	4	2	69,0	71,6	72,9	72,4	72,8	71,2	72,3	70,3	71,2	8142
Two Layers	16	1	68,6	69,1	71,2	72,4	69,1	68,6	60,7	70,3	72,8	4096
Two Layers	16	2	69,5	68,6	71,6	73,2	70,0	69,9	66,1	70,3	72,8	2048
Two Layers	16	4	69,9	69,5	73,3	72,8	71,2	70,0	67,0	69,5	71,6	1024
Two Layers	16	8	68,6	67,4	72,0	70,8	71,1	68,7	67,0	70,3	70,8	512
Two Layers	16	16	63,6	66,5	69,9	70,7	68,3	66,6	64,4	68,2	66,5	256

HRF MVPA. After convolving with the HRF, resulting response matrix is used in a similar way with Raw MVPA. Second, we considered a 6 sample time window after a stimulus and concatenated all the intensity values obtained during that period, which we called Temporal MVPA (T-MVPA). This process yields a single feature vector for each sample which is 6 times larger than MVPA and HRF MVPA.

The proposed method and compared approaches are trained independently for each of eight runs, for nine subjects and the final result for a subject is averaged over runs. Moreover, we conducted a binomial tests to measure significance of our proposed model results against randomness. We considered the null hypothesis that the classifier was performing at chance level (10% for general, 50% for one-vs-all fashion). The largest p-value the tests yielded was 0.0004 and the null hypothesis was rejected.

## 4 RESULTS

In this section, we present and analyse the performance results of the proposed approach. Experimental results are analysed by considering final feature space dimensions (last column of Table I) in classifiers by comparing classification accuracies. Overall results are also illustrated in Table 1. For the classical and temporal MVPA approaches, Raw MVPA approach is taken as baseline method. HRF convolved MVPA model performed poorly compared to Raw MVPA results only in two subjects (indicated by Sub) and improved performance up to 8% for the rest of the participants. This is expected as we employ temporal information but without adjusting HRF to the data regularities, rather hand-crafted. Similarly T-MVPA method use temporal information without any HRF assumption and improves performance compared to other MVPA methods.

Proposed temporal CNN architecture is tested with varying depth (single layer and two layer rows in Table 1) and pooling ranges ( $\delta_1$  and  $\delta_2$  columns). A single layer (shallow) temporal feature learning and convolution architecture with varying pooling range between 2 to 16 yields in a feature space with dimensions from 8192 to 1024. For all nine subjects, single layer architecture outperforms classical and temporal MVPA methods substantially, up to 60%. By appropriate pooling, the feature dimensions of the single layer architecture retracted to 1024 where we still observe 20% improvement. In order to analyse the impact of the depth and further reduce feature dimensionality, two layer architecture is tested with varying pooling ranges in the second level. The proposed model in two layers reduces feature dimensions down to 256 where we still observe better performance in 8 subjects compared to the single layer architecture with lowest dimensions. The results suggest that employing temporal structures for brain decoding gives rise to better classification accuracies. Hierarchical convolutional models pre-trained with a slightly larger amount of unlabelled data are appropriate candidates to employ temporal information in an efficient way. Furthermore, increasing depth of such temporal convolutional architectures makes it possible to reduce feature dimensionality, and the learned filters become more complex and non-linear resulting a better performance.

## 5 CONCLUSION

In this paper, we have considered a novel approach for brain decoding for fMRI data using unsupervised feature learning and convolutional neural networks. By leveraging unlabelled data and multi-layer temporal CNNs, we learn multiple layers of temporal filters which represent the activation patterns of voxels under experimental conditions. By making use of deep temporal representations, we train powerful and robust brain decoding models. This represents a departure from previous classical MVPA approaches which generally relied on raw voxel intensity values. As evidence of the power of proposed model, we conducted a recognition memory experiment on 9 subjects and observed significant performance improvements. The proposed model has potential to further improvements by incorporating spatial structures with spatial convolution and pooling, which is left as a future work.

### ACKNOWLEDGMENTS

Authors thank all Beyincik members for insightful discussions on fMRI data pre-processing. This work is supported by TUBITAK Project, 112E315.

### REFERENCES

Battle, Alexis, Chechik, Gal, and Koller, Daphne. Temporal and cross-subject probabilistic models for fmri prediction tasks. In *NIPS*, volume 6, pp. 121–128, 2006.

Bengio, Yoshua and LeCun, Yann. Scaling learning algorithms towards AI. In *Large Scale Kernel Machines*. MIT Press, 2007.

Bengio, Yoshua, Courville, Aaron, and Vincent, Pascal. Representation learning: A review and new perspectives. *IEEE Transactions on Pattern Analysis and Machine Intelligence*, 35(8):1798–1828, 2013. ISSN 0162-8828.

Erhan, Dumitru, Bengio, Yoshua, Courville, Aaron, Manzagol, Pierre-Antoine, Vincent, Pascal, and Bengio, Samy. Why does unsupervised pre-training help deep learning? *J. Mach. Learn. Res.*, 11:625–660, March 2010. ISSN 1532-4435.

Haynes, John-Dylan and Rees, Geraint. Decoding mental states from brain activity in humans. *Nature reviews. Neuroscience*, 7, 2006.

Hinton, Geoffrey E., Osindero, Simon, and Teh, Yee Whye. A fast learning algorithm for deep belief nets. *Neural Computation*, 18:1527–1554, 2006.

Kavukcuoglu, Koray, Ranzato, M, Fergus, Rob, and LeCun, Yann. Learning invariant features through topographic filter maps. In *IEEE Conference on Computer Vision and Pattern Recognition (CVPR)*, pp. 1605–1612, 2009.

Krizhevsky, Alex, Sutskever, Ilya, and Hinton, Geoffrey E. Imagenet classification with deep convolutional neural networks. In *Advances in Neural Information Processing Systems*, pp. 2012.

Le, Quoc V, Zou, Will Y, Yeung, Serena Y, and Ng, Andrew Y. Learning hierarchical invariant spatio-temporal features for action recognition with independent subspace analysis. In *IEEE Conference on Computer Vision and Pattern Recognition (CVPR)*, pp. 3361–3368, 2011.

Mitchell, Tom M, Shinkareva, Svetlana V, Carlson, Andrew, Chang, Kai-Min, Malave, Vicente L, Mason, Robert A, and Just, Marcel Adam. Predicting human brain activity associated with the meanings of nouns. *Science*, 320(5880):1191–1195, 2008.

Norman, Kenneth A, Polyn, Sean M, Detre, Greg J, and Haxby, James V. Beyond mind-reading: multi-voxel pattern analysis of fMRI data. *Trends in cognitive sciences*, 10, 2006.

Oztekin, Ilke and Badre, David. Distributed Patterns of Brain Activity that Lead to Forgetting. *Frontiers in human neuroscience*, 5, 2011.

Pereira, Francisco and Botvinick, Matthew. Information mapping with pattern classifiers: a comparative study. *Neuroimage*, 56(2):476–496, 2011.

Raina, Rajat, Battle, Alexis, Lee, Honglak, Packer, Benjamin, and Ng, Andrew Y. Self-taught learning: transfer learning from unlabeled data. In *Proceedings of the 24th international conference on Machine learning*, pp. 759–766, 2007.

Shirer, W R, Ryali, S, Rykhlevskaia, E, Menon, V, and Greicius, M D. Decoding subject-driven cognitive states with whole-brain connectivity patterns. *Cerebral cortex (New York, N.Y. : 1991)*, 22(1):158–65, January 2012. ISSN 1460-2199.

Sidhu, Gagan S, Asgarian, Nasimeh, Greiner, Russell, and Brown, Matthew R G. Kernel principal component analysis for dimensionality reduction in fmri-based diagnosis of adhd. *Frontiers in Systems Neuroscience*, 6(74), 2012. ISSN 1662-5137.

Viviani, Roberto, Grön, Georg, and Spitzer, Manfred. Functional principal component analysis of fmri data. *Human brain mapping*, 24(2):109–129, 2005.